Drilling scheme analysis and output prediction of instrumented wheel-set based on Finite Element Method and LSTM

Shuangxi Chen [1, a,*], Songlin Jiang [2, b], Haitao Man [2,c]

[1] Chengdu University Chengdu, China

[2] Chengdu Dayun Automobile Co.Ltd. Chengdu, China

[*, a] chenshuangxi@cdu.edu.cn, [b] jsl87919@163.com, [c] 553720089@qq.com

Abstract. Based on the Finite Element Method and wheel-rail force measurement theory, the effects of different drilling schemes and parameters on the output of the measuring electrical bridge are analyzed, and the optimal parameters are determined. The finite element model of a metro instrumented wheel-set is established by software ABAQUS. The effects of drilling radius, hole size and wheel-rail contact point on the strain of measuring points are calculated and analyzed, and the measuring bridge outputs of two different drilling schemes are compared. The output of the wheel-rail forces is predicted based on LSTM long short memory network. The results show that: (1) the optimal drilling position is on the middle surface of the wheel, (2) The drilling scheme of eight-hole is better than that of four-hole, (3) LSTM neural network can realize decoupling of bridge signal and high precision prediction of wheel-rail forces.

Keywords: Instrumented wheel-set, finite element analysis, drilling scheme, LSTM neural network

1. Introduction

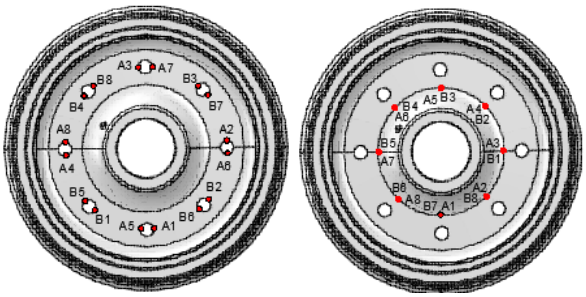
When the train is running on the line, the wheel rail contact behavior exists in the normal direction and tangent direction of the contact surface. According to the theory of wheel rail contact mechanics, there is Hertz contact force in the normal direction and creep force (moment) in the tangential direction. Decompose the Hertz contact force and creep force (moment) in the track coordinate system to obtain the wheel rail vertical force, transverse force and longitudinal force. According to Chinese standard GB/T 5599-2019 for dynamic performance evaluation and test evaluation of rolling stocks, the derailment coefficient and wheel load reduction rate of rolling stocks are the function of wheel rail vertical force and transverse force. Therefore, accurate measurement of wheel rail force is important for safety evaluation of train.

Wheel-rail force measuring methods are divided into two categories: direct method and indirect method. The instrumented wheel-set is the direct measurement method with the highest measurement accuracy at present. As early as the 1980s, China has developed spoke plate contact instrumented wheel-set. Chen Chengyuan [1] introduced the method of selecting the best patch location and the principle of bridge design. Wu Duo [2] put forward the iterative method of data processing of instrumented wheel-set. Zeng Yuqing[3]established the corresponding strain analysis and bridge formation theoretical system of spoke wheel, and gave a new method of contact measurement of instrumented wheel-set. Liu Shangju[4] introduced the method of improving the sensitivity of measuring bridge and reducing noise. Shao Yuping [5] proved that BP neural network was applied to the decoupling of vertical and horizontal electric bridge of force measuring wheel-set. Chang Chongyi[6]used the finite element software to analyze the force of the force measuring wheel-set, find the best patch position, and shorten the design and calibration cycle. In 2010, Japan Railway Comprehensive Technology Research Institute newly developed intermittent and continuous instrumented wheel-set test and processing system [7]. Chu Gaofeng[8] evaluated the influence of centrifugal force on the measurement error of force measuring wheel-set of high-speed train by using finite element technology. Chen Shuangxi [9] used empirical mode decomposition and finite element method to compare and analyze the signal output characteristics of different bridges. Vahid Reza Bagheri [10] proposed an optimization scheme of strain gauge patch on the spoke surface. Su Jianqiu [11] decoupled the Kalman filter method from the measured signal of the instrumented wheel-set.

In this study, two drilling schemes of the instrumented wheel-set of a type of subway train are designed and studied. The influence of drilling position, hole parameters and contact point position on the output of the bridge is analyzed by using the finite element simulation technology, and the best design parameters are determined. The output difference between the two drilling schemes is compared. The output of the instrumented wheel-set is also predicted by using the long and short memory neural network (LSTM).

2. Drilling and bridge scheme of instrumented wheel-set

The design of instrumented wheel-set of metro train is shown in Fig.1. The drilling method of spoke plate can be designed as eight-hole and four-hole. The drilling position is arranged in an array on the circumference with radius R (mm), and the diameter of the hole is d (mm). The elastic analysis shows that when the wheel-set tread is subjected to vertical force, the maximum radial stress on the wheel-set spoke surface is located on the inner surface of the hole. Therefore, the strain gauge is symmetrically installed on the inner surface of the hole along the radial direction. The measuring point position of the four-hole scheme is similar to that of the eight-hole scheme, which is omitted here. The vertical and transverse bridge schemes of the instrumented wheel-set are shown in Fig.2 and Fig.3. Different from the vertical force measurement bridge patch method, the strain gauge of the transverse force measurement bridge is pasted at the root of the spoke surface. Strain gauges A1~ A8 form bridge A of vertical/transverse bridge, and strain gauges B1~B8 form bridge B. In the bridge A (B) of the vertical bridge, the strain gauges A1 (B1) and A3 (B3), A5 (B5) and A7 (B7), A2 (B2) and A6 (B6), A4 (B4) and A8 (B8) are the four bridge arms of the vertical measuring bridge respectively. In the bridge A (B) of the transverse bridge, the strain gauges A1 (B1) and A2 (B2), A3 (B3) and A4 (B4), A5 (B5) and A6 (B6), A7 (B7) and A8 (B8) are the four bridge arms of the transverse measuring bridge respectively. The bridge design of the four-hole scheme is similar to the eight-hole scheme, which is omitted here.



(a)Vertical bridge (b)Transverse bridge

Fig. 1. The scheme of drilling and the position of measuring point

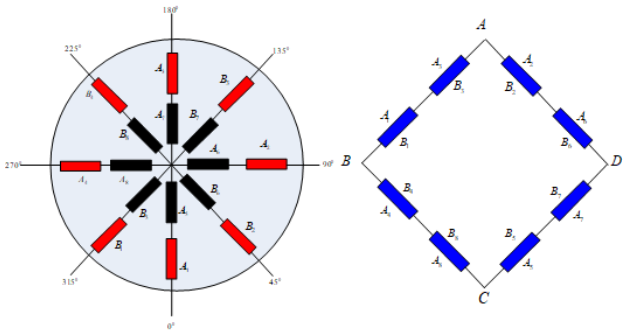


Fig. 2. Wheel-rail vertical force measuring bridge

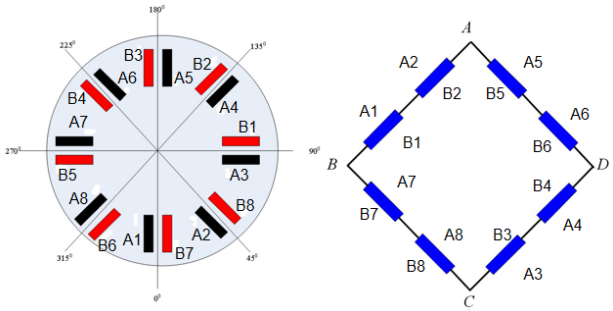


Fig. 3. Wheel-rail lateral force measuring bridge

The output of Wheatstone bridge is usually proportional to the actual output of Wheatstone bridge. The strains of opposite bridge arm in Fig.2 and Fig.3 are added, and the strains of adjacent bridge arm are subtracted. Therefore, the output of bridge A for vertical force measurement is

$$V_A = \frac{1}{4} KE[(\varepsilon_{A1} + \varepsilon_{A3} + \varepsilon_{A5} + \varepsilon_{A7}) - (\varepsilon_{A2} + \varepsilon_{A6} + \varepsilon_{A4} + \varepsilon_{A8})] \tag{1}$$

The output of bridge A for transverse force is

$$U_A = \frac{1}{4} KE[(\varepsilon_{A1} + \varepsilon_{A2} + \varepsilon_{A3} + \varepsilon_{A4}) - (\varepsilon_{A5} + \varepsilon_{A6} + \varepsilon_{A7} + \varepsilon_{A8})] \tag{2}$$

Where K and E are constants related to sensor, ε_{Ai} (i = 1 ~ 8) is strain. The output formulas of vertical and transverse bridge B are similar.

The combined output of transverse force bridge U_{AB} and vertical force bridge V_{AB} is only related to the magnitude of transverse force and vertical force, and has a linear relationship, but has nothing to do with the rotation angle of wheel-set.The bridge output formula is as follows

$$U_{AB} = \sqrt{U_A^2 + U_B^2} \tag{3}$$

$$V_{AB} = |V_A| + |V_B| \tag{4}$$

3. Simulation and analysis of bridge output

3.1 Finite element model of instrumented wheel-set

In this study, the finite element model is established according to the CAD drawing of a metro train wheel-set, as shown in Fig.4. To ensure enough calculation accuracy, the wheel is meshed with hexahedron. The length of the mesh is 10mm. There are 429711 meshes in the whole model. The wheel-set axle assembly is fully constrained, and a moving concentrated force load is applied on the tread to simulate the change of the position of the wheel rail contact point. The load is arranged at equal intervals of 1 degree on the circumference of the rolling circle and is divided into 360 load steps, which can simulate the change of strain of the measuring point during the wheel rail force rotates on the wheel tread for one cycle. The parametric loading program is written based on ABAQUS secondary development module, which can realize rapid automatic calculation and analysis. After calculating the strain, the output of the measuring bridge can be calculated according to equations(1) ~ (4).

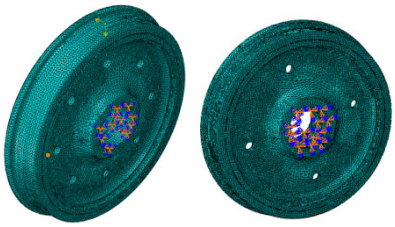


Fig. 4. Finite element model of instrumented wheel-set

3.2 Analysis of drilling scheme

The influence of position radius *R* and hole diameter *d* should be considered for the hole size of spoke surface. Through finite element analysis, the optimal position on radius *R* and hole diameter *d* can be determined. The calculation results of the influence of hole position radius are shown in Fig.6. When the radius R of the hole position is increased from 220mm to 290mm, the micron strain of the patch position in the hole increases from 175 to 223. When the radius R of the hole position is increased from 220mm to 250mm, the radial micron strain at the root of spoke surface increases rapidly from 60 to 260. When R increases from 250mm to 290mm, the radial micron strain increases from 264 to 299, but the increasing trend is slow. There is little difference between the inside and outside. The optimum range of hole position radius *R* is 250mm~290mm. Therefore, holes can be drilled in the middle of the surface, that is, *R* can be designed as 260mm.The calculation results show that when the hole diameter *d* increases from 20mm to 60mm, the micron strain of the position in the hole decreases slowly from 200 to 194, and the radial micro strain at the root of surface decreases from 291 to 251. Therefore, within the reasonable range, the influence of hole size on hole strain is limited, and *d* can be designed as 40mm.The influence of the wheel rail contact point on the strain of the measuring point is shown in Fig.6. Set the rolling circle position y = 65mm, the wheel rail contact point is within the range of 45mm ~ 105mm, and the radial strain at the root of the surface changes little. When the contact point of wheel rail is at the rolling circle, the radial strain on the inner wall of the hole has a minimum. When the contact point of wheel rail is at the wheel flange, the radial strain of the hole has a maximum value. Therefore, the position of the contact point has limited influence on the position strain of the measuring point and less influence on the output of the bridge.

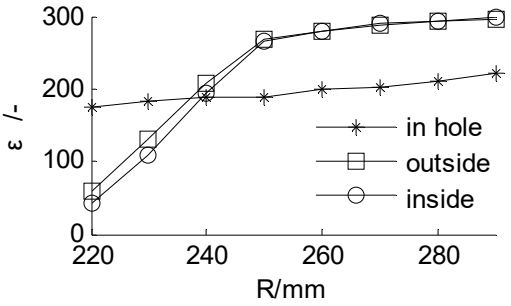


Fig. 5. Curve of radial strain with radius *R*

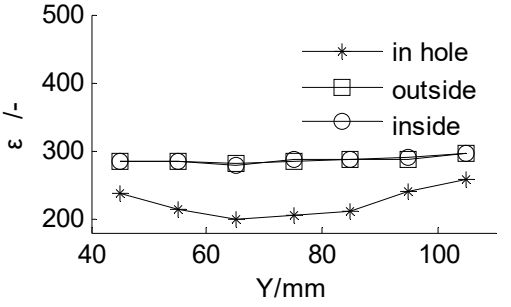


Fig. 6. Curve of radial strain with contact point

3.3 Analysis of bridge construction scheme

The outputs of vertical and transverse bridge are shown in Fig.7 and Fig.8 respectively. When the 8-hole scheme is adopted, the output amplitude fluctuation of both vertical bridge and transverse bridge is small. If the 4-hole scheme is adopted, the output of the vertical bridge is a triangular wave with large amplitude, but the output amplitude fluctuation of the transverse bridge is small. Therefore, the 8-hole scheme is suggested for the instrumented wheel-set, since its output amplitude fluctuation is much smaller than that of 4-hole scheme.

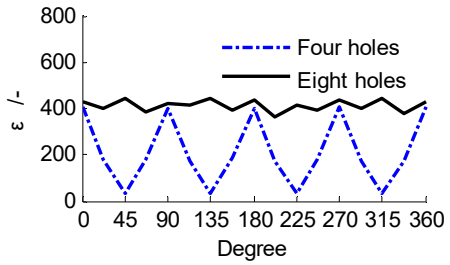


Fig. 7. Vertical bridge output comparison

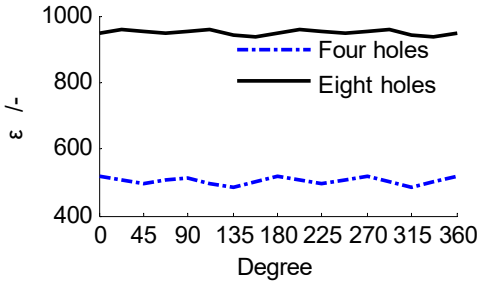


Fig. 8. Transverse bridge output comparison

4. wheel rail force Prediction

4.1 LSTM neural network

In recent years, the rapid development of deep learning artificial intelligence technology provides a new tool for the decoupling of vertical force and transverse force and the prediction of output signal. Based on the output signal of the instrumented wheel-set bridge above, the wheel rail force prediction is realized by applying the long short memory neural network (LSTM) proposed by Hochreater and Schmidhuber [12]. LSTM model is an improved model of recurrent neural network (RNN), which has solved the inherent problems of gradient explosion and gradient disappearance of RNN model, and becomes an effective prediction tool for time series and nonlinear data flow. The unit model of LSTM is shown in fig. 9, which is characterized by controlling the information state at each time in the neural network through the gates (forgetting gate, input gate and output gate), realizing its special long-term and short-term data memory function, making the model more suitable for learning the characteristics of correlated and continuous data. The calculation formulas [12,13] of forgetting gate f_t, input gate i_t, unit memory signal C_t ($\widetilde{C_t}$), output o_t and h_t at time t are as follows:

$$f_t = \sigma\left(W_f \times [h_{t-1}, x_t] + b_f\right) \tag{5}$$

$$i_t = \sigma(W_i \times [h_{t-1}, x_t] + b_i) \tag{6}$$

$$o_t = \sigma(W_o \times [h_{t-1}, x_t] + b_o) \tag{7}$$

$$\widetilde{C_t} = tanh(W_c \times [h_{t-1}, x_t] + b_c) \tag{8}$$

$$h_t = o_t \tanh\,(C_t) \tag{9}$$

$$C_t = f_t C_{t-1} + i_t \widetilde{C_t} \tag{10}$$

Where W_f、W_i、W_o 、W_c are the weight matrix of each gate node, b_f、b_i、b_o、b_c are the offset of each gate node, σ is the sigmod function and $tanh$ is the hyperbolic tangent function.

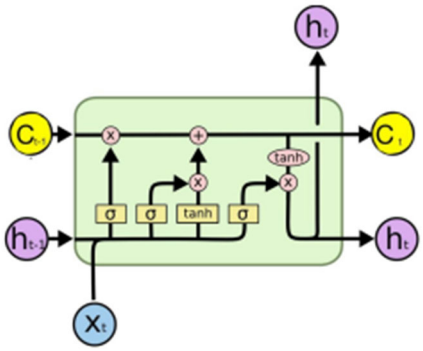


Fig. 9. Unit structure diagram of LSTM

4.2 Wheel-rail force prediction

Based on the above finite element model, load cases are determined according to the actual engineering, the simulation is completed by ABAQUS software, the input and output signals of the system were obtained, and LSTM was applied to predict the wheel-rail force. Eight strain signals (ε_{Ai} 、 ε_{Bi}) of bridge A and bridge B of vertical/ transverse bridge are input data, and the output are wheel-rail vertical force Q and transverse force Y. According to the test experience, vehicle parameters, and the dynamic response, the wheel-rail vertical force is assumed in the range of 0 ~ 150 kN and lateral force from -100kN to 100 kN. The training and test samples are obtained by using the parametric finite element modeling, simulation and analysis of ABAQUS software. To gain the predicted output of wheel/rail force, the response of strain gauge in Fig. 3 and Fig. 4 is used as the input of LSTM model, and the wheel rail force load is the output of the model. The prediction results of wheel-rail vertical force and transverse force of typical eight-hole bridge are shown in Fig.10 and Fig.11. The predicted results of lateral and vertical force are completely consistent with the theoretical results, and the relative error is less than 1%. The relative error of vertical force is slightly larger than that of transverse force. Therefore, the LSTM neural network can realize the decoupling of bridge signal and high precision prediction of wheel-rail force.

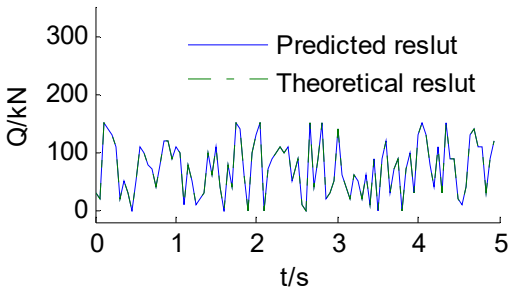


Fig. 10. LSTM prediction of wheel-rail vertical force

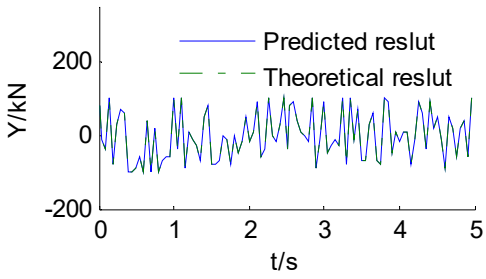


Fig. 11. LSTM prediction of wheel-rail transverse force

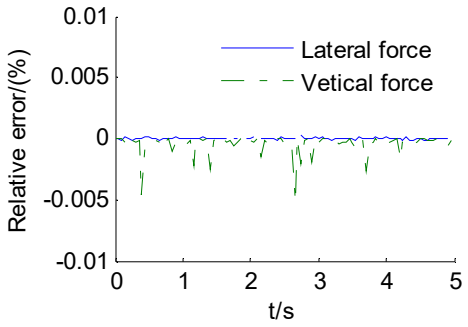


Fig. 12. Relative error of wheel-rail force prediction

References

[1] Chen Chengyuan, Shi Yan. Instrumented wheel-settechnique for continuous meaurement of wheel/rail loads[J]. Journal of southwest jiaotong university, 1994, 29(3):263-267.

[2] Wu Duo, Luo HongKui. Using Iterative Method to Process the Data Measured by Instrument Wheelset[J]. China Railway Science, 1994, 29(3):263-267.

[3] Zeng Yuqing, Wang Weidong, Gan Dunwen. Theory of High Accuracy Load Measuring Wheelset[J]. Journal of the China Railway Society,1998, (6):28.

[4] Liu Shangju, Jin Xuesong, Zhang Limin.Research for Improving the Measurement Accuracy of the Instrumented Wheelset[J]. Rolling Stock,1998(02):32-34.

[5] SHAO Yuping, CHEN Jianzheng. Application Study on BP Neural Network Applied to Calculation about a Instrumented wheel-setwith Horizontal and Vertical Bridge Combination[J]. Railway Locomotive & Car, 2003, 29(5):36-38.

[6] Chang Chongyi, Wang Chengguo, Li Lan. Study on Numerical Test of Instrumented wheel-setfor Continuous Measurement[J]. Railway Locomotive & Car, 2007, 27(5): 3-5.

[7] Zuo Tengjie, Liu Yangchun. Development of Wheel Load and Lateral Force Measurement Processing System Combining Intermittent and Continuous Measurement Methods[J]. Foreign Rolling Stock, 2010(01):32-37.

[8] Chu Gaofeng, Li Gu, Zu Honglin. Finite Element Analysis on the Instrumented wheel-setof High Speed EMU[J]. Railway Locomotive & Car,2011, 31(1):90-93.

[9] Chen Shuangxi, Lin Jianhui, Chen Jianzheng. Comparison of electrical bridge behaviors of an instrumented wheel-setbased on improved EMD and FEM[J]. Journal of vibration and shock, 2012, 31(6): 131-135.

[10] Bagheri V R, Tehrani P H, Younesian D. Optimal strain gauge placement in instrumented wheel-setfor measuring wheel-rail contact forces[J]. International Journal of Precision Engineering and Manufacturing, 2017, 18(11):1519-1527.

[11] Su Jianqiu, Chen Jianzheng. Wheel/rail force calculation based on UKF-KF[J]. Electronic Measurement Technology, 2018(14): 55-58.

[12] HOCHREITER S, SCHMIDHUBER J. Long Short-term Memory [J]. Neural Computation,1997,9(8): 1735-1780.

[13] Lei Jinhao, Liu Chao, JIANG Dongxiang. Fault Diagnosis of Wind Turbine Based on Long Short-term Memory Networks [J]. Renewable Energy, 2019, 133: 422-432.